Wavelength Division Demultiplexing of Nyquist WDM Signals under Frequency Offset and Receiver-side IQ Impairments

Takuma Kuno, Yojiro Mori, Hiroshi Hasegawa

Nagoya University, kuno.takuma.g2@s.mail.nagoya-u.ac.jp

Abstract *The interaction among wavelength division demultiplexing (WDD), frequency offset estimation, and receiver-side IQ impairment compensation in Nyquist WDM systems is reported for the first time. We propose a novel WDD scheme effective against such interactive impairments and demonstrate its performance through proof-of-concept transmission experiments.*

Introduction

Nyquist wavelength-division-multiplexing (WDM) systems can realize ultimate spectral efficiency while avoiding inter-symbol interference (ISI) and inter-channel crosstalk [1-3]. Nyquist WDM signals need to be demultiplexed by digital filters having steep cut-off characteristics. In the presence of the frequency offset, the frequency discrepancy between the transmitter laser and local oscillator, a non-adaptive filter eliminates a part of the target channel spectrum and passes a part of its adjacent-channel spectrum. Thus, the signal is impaired by ISI and inter-channel crosstalk in the process of wavelength division demultiplexing (WDD). Although adaptive filters can demultiplex Nyquist-WDM signals with the frequency offset, such filters must have long-delay taps to attain steep cut-off characteristics.

This background yielded the basic WDD framework for Nyquist WDM systems [4]. The concept is to shift the passband frequency of the WDD filter according to the frequency offset value obtained by the frequency offset estimator. The estimation of the frequency offset is conducted after coarse WDD and polarization recovery with adaptive filters having short-delay taps. With this scheme, the target channel can be extracted with the sharp cut-off filters under the frequency offset. However, this WDD framework fails when the signal simultaneously suffers from frequency offset and receiver-side IQ impairments including IQ skew, IQ-power mismatch, and IQ-phase mismatch. This interaction causes crosstalk and has already been discussed for digital sub-carrier multiplexing systems [5-9]; the crosstalk can be eliminated by multiple-input multiple-output processing using multiple sub-carriers within the same channel [6,7]. In Nyquist WDM systems, however, a part of the adjacent channel spectra is diminished by the analogue filter in the receiver. Consequently, the same scheme cannot be applied to Nyquist WDM systems.

In this paper, we propose, for the first time, a novel WDD scheme that can handle the interactive impairments inherent in Nyquist WDM systems. We first elucidate the interaction of the frequency offset and receiver-side IQ impairments, which occurs in the WDD process. Afterwards, the performance of the proposed scheme is experimentally shown. No notable degradation is observed in the proof-of-concept experiments assuming Nyquist WDM systems.

Principle of WDD in Nyquist WDM Systems

WDD under Frequency Offset

To demultiplex Nyquist WDM signals under an arbitrary frequency offset, the passband frequency of the WDD filter must be altered to suit the frequency offset. Fig. 1 shows the concept of the WDD framework for Nyquist WDM systems [4]. This scheme enables the receiver to extract the target signal by adjusting the passband frequency of the WDD filter according to the output of the frequency-offset estimator. Since remnants of the adjacent channel disturb the operation of the adaptive filters for polarization division demultiplexing, the WDD filter should precede the adaptive filters.

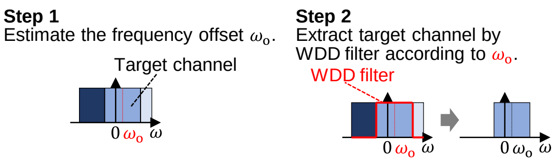

Fig. 1: Concept of the frequency-offset-adaptive WDD.

WDD under Frequency Offset and Receiver-side IQ Impairments

The interaction of frequency offset and receiver-side IQ impairments causes crosstalk within the Nyquist WDM signal. The spectrum of the received signal under frequency offset ω_o is given by

$$S(\omega)=S_L(\omega-\omega_o)+S_T(\omega-\omega_o)+S_R(\omega-\omega_o), \quad (1)$$

where $S_L(\omega)$, $S_T(\omega)$, and $S_R(\omega)$ represent the spectrum on the left side of the target signal spectrum, the spectrum of the target signal, and the spectrum on the right side of the target signal, respectively. Here, we assume that a part of $S_L(\omega)$ and $S_R(\omega)$ are diminished by the analogue filter in the receiver. The widely linear (WL) model

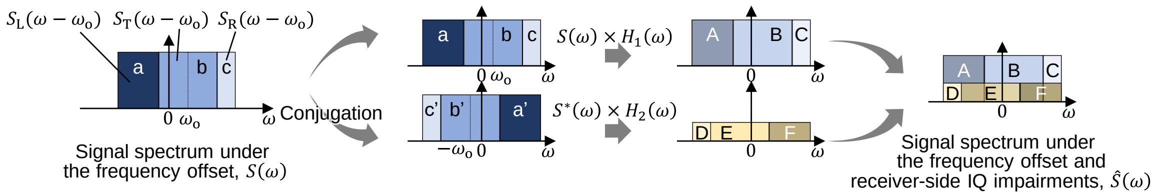

Fig. 2: Crosstalk occurrence process due to the interaction between the frequency offset and receiver-side IQ impairments.

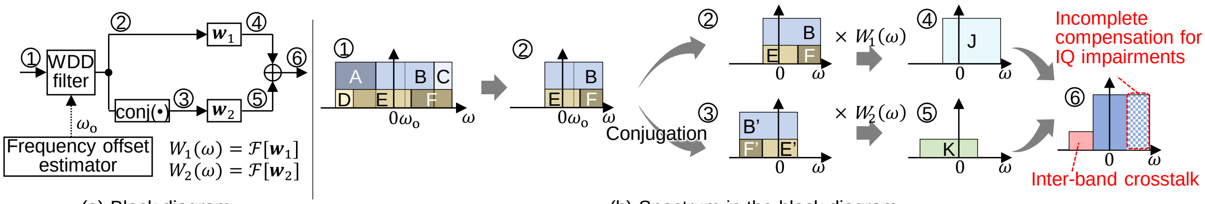

(a) Block diagram.

(b) Spectrum in the block diagram.

Fig. 3: Straightforward process of WDD and WL equalization.

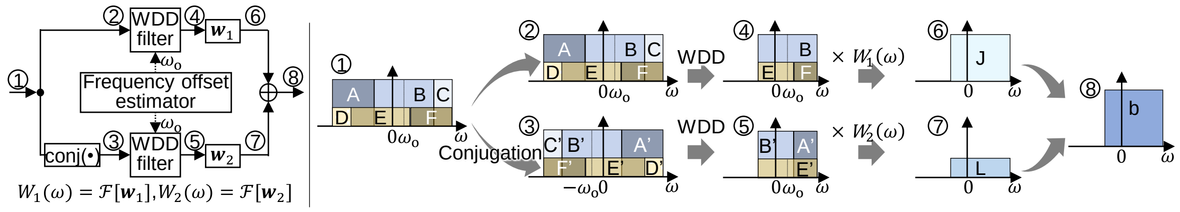

(a) Block diagram.

(b) Spectrum in the block diagram.

Fig. 4: Proposed process of WDD and WL equalization.

describes the signal spectrum including receiver-side IQ impairments by

$$\hat{S}(\omega) = H_1(\omega)\, S(\omega) + H_2(\omega)\, S^*(\omega), \qquad (2)$$

where $H_1(\omega)$ and $H_2(\omega)$ are complex numbers that express receiver-side IQ impairments [10]. Fig. 2 shows the origin of the crosstalk under both frequency offset and receiver-side IQ impairments. The signal spectrum originating from the complex conjugate overlaps on the target channel spectrum and becomes crosstalk. The crosstalk can be eliminated through WL equalization given by

$$W_1(\omega)\hat{S}(\omega) + W_2(\omega)\hat{S}^*(\omega) = S(\omega), \qquad (3)$$

where $W_1(\omega)$ and $W_2(\omega)$ are $\frac{H_1{}^*(\omega)}{|H_1(\omega)|^2-|H_2(\omega)|^2}$ and $\frac{H_2(\omega)}{|H_2(\omega)|^2-|H_1(\omega)|^2}$, respectively.

The WDD function needs to precede the adaptive filters to ensure stable operation. However, if the WDD filters and the WL filters are straightforwardly connected as shown in Fig. 3(a), a part of the inter-band crosstalk remains in the output as shown in Fig. 3(b). In addition, receiver-side IQ impairments can never be fully compensated due to the lack of necessary signal components for WL equalization.

To realize WDD while compensating receiver-side IQ impairments simultaneously, WDD for the received signal and its complex conjugate must be done independently. Fig. 4(a) shows the concept of the proposed WDD scheme. The transition of spectral overlap is shown in Fig. 4(b). The received signal and its complex conjugate are processed by the WDD filters before WL equalization. The WDD filters have the same passband frequency, and their centre frequency is shifted according to the estimated frequency offset value. This scheme can eliminate inter-channel crosstalk and the crosstalk caused by the interaction between the frequency offset and receiver-side IQ impairments.

Experiments

We measured bit-error ratios (BERs) of 3-ch 32-Gsymbol/s DP 16QAM signals to evaluate the performance of the proposed WDD scheme, where the guardband bandwidth is set to 1 GHz considering frequency stability of the lasers adopted. Fig. 5 shows the experimental setup. We used external-cavity lasers (ECLs) whose linewidths were 100 kHz. The target signal and the non-target signals were formed independently with two IQ modulators driven by an arbitrary waveform generator (AWG), which generated 4-level Nyquist-shaped IQ signals. Polarization division multiplexing (PDM) was conducted in split-delay-combine manner. The target and non-target channels were combined by a 2×1 optical coupler. This yielded 3-ch Nyquist WDM 32-Gsymbol/s DP 16-QAM signals.

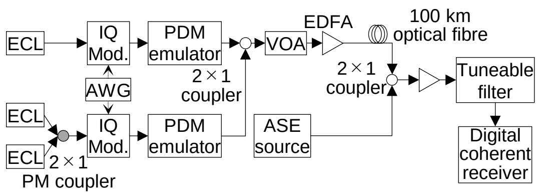

Fig. 5: Experimental setup.

The total optical power of the three WDM was adjusted with a variable optical attenuator (VOA). After 100 km transmission through optical fibre, amplified spontaneous emission (ASE) noise was loaded onto the signals. Finally, the signals were filtered, pre-amplified, and coherently detected. The passband of the anti-aliasing filters was 23 GHz. Sampling rate of the analogue-to-digital converter was 50 Gsample/s. The digitized signal was then input to our digital signal processing (DSP) circuit, see Fig. 6. Our DSP circuit consisted of seven layers of filters. The red processing blocks/lines correspond to newly added/modified functions compared to the state-of-the-art multi-layer filter reported in 2022 [11]. We parameterized frequency offset and receiver-side IQ skew. We compared four demodulation schemes as detailed in Tab. 1.

Fig. 7 shows bit-error ratio (BER) performance of the centre channel as a function of the frequency offset, where receiver-side IQ skew was set to 0 s. All BERs in scheme A are worse. This is because the cut-off characteristics of short-delay-tap filters are blunt compared to the WDD filter. Scheme B offers the best BER only when the frequency offset is 0 Hz; its performance is seriously degraded if frequency offset is present. Schemes C and D offer the best performance irrespective of the frequency offset.

Fig. 8 shows BER measured as a function of receiver-side IQ skew, where the frequency offset is also parametrized. Scheme A shows unstable operation and all BERs are worse due to the large inter-channel crosstalk. Scheme B yields the best performance only when the frequency offset is 0 Hz. Scheme C suffers performance degradation when the frequency offset and the receiver-side IQ impairments coexist. Scheme D, which is our proposed scheme, suffers no notable penalty even if the frequency offset and the receiver-side IQ impairments are present. In this way, the proposed scheme can eliminate the crosstalk created by the interaction between the frequency offset and receiver-side IQ skew.

Conclusions

We elucidated the principle of the interaction of WDD, frequency offset estimation, and receiver-side IQ impairment compensation in Nyquist WDM systems. The proposed WDD scheme in conjunction with other advanced DSP functions can offset the combined system impairments. Experiments showed that the proposed scheme yielded the best performance with no notable penalty.

Acknowledgements

This research and development work was supported by JSPS/KAKENHI (JP22J23852) and MIC/SCOPE (JP192106002)

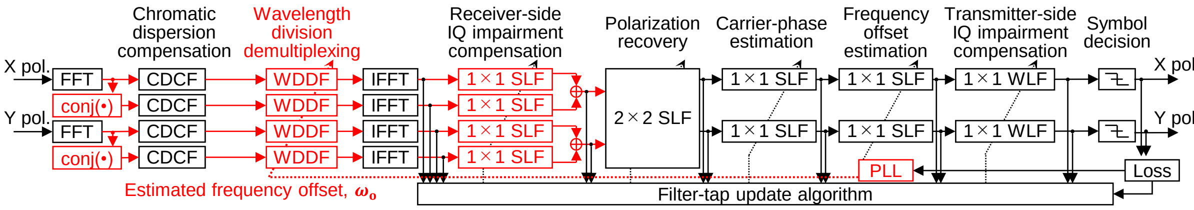

Fig. 6: Configuration of the DSP circuit. (SLF: strictly linear filter and WLF: widely linear filter).

Tab. 1: Tested schemes.

Scheme	DSP configuration
A	Multi-layer filter [11] without WDD filter
B	Multi-layer filter [11] with non-adaptive WDD filter
C	Multi-layer filter [11] with WDD filter straight-forwardly adaptive to frequency offset
D	**Proposed DSP configuration shown in Fig. 6**

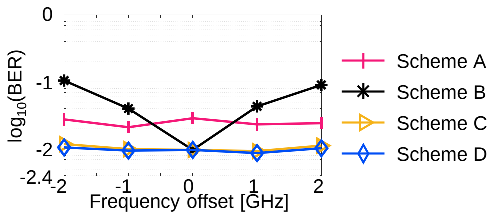

Fig. 7: Measured frequency offset tolerance without IQ impairments.

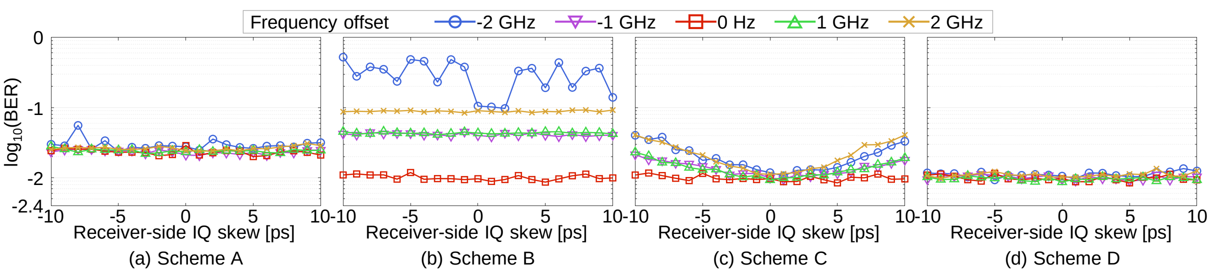

Fig. 8: Measured tolerance for receiver-side IQ impairments and the frequency offset.

References

[1] G. Bosco, V. Curri, A. Carena, P. Poggiolini, and F. Forghieri, "On the performance of Nyquist-WDM terabit superchannels based on PM-BPSK, PM-QPSK, PM-8QAM or PM-16QAM subcarriers," *Journal of Lightwave Technology*, vol. 29, no. 1, pp. 53-61, 2011, DOI: 10.1109/JLT.2010.2091254.

[2] R. Schmogrow, M. Winter, M. Meyer, D. Hillerkuss, S. Wolf, B. Baeuerle, A. Ludwig, B. Nebendahl, S. Ben-Ezra, J. Meyer, M. Dreschmann, M. Huebner, J. Becker, C. Koos, W. Freude, and J. Leuthold, "Real-time Nyquist pulse generation beyond 100 Gbit/s and its relation to OFDM," *Optics Express*, vol. 20, no. 1, pp. 317-337, 2012, DOI: 10.1364/OE.20.000317.

[3] X. Zhou, L. E. Nelson, P. Magill, R. Isaac, B. Zhu, D. W. Peckham, P. I. Borel, and K. Carlson, "PDM-Nyquist-32QAM for 450-Gb/s per-channel WDM transmission on the 50 GHz ITU-T grid," *Journal of Lightwave Technology*, vol. 30, no. 4, pp. 553-559, 2012, DOI: 10.1109/JLT.2011.2177243.

[4] Y. Mori, C. Han, H. Lu, and K. Kikuchi, "Wavelength demultiplexing of Nyquist WDM signals under large frequency offsets in digital coherent receivers," *in Proceedings European Conference and Exhibition on Optical Communication (ECOC 2013)*, London, UK, 2013, paper Mo.4.C.6, DOI: 10.1049/cp.2013.1313.

[5] T. Duthel, C. R. S. Fludger, B. Liu, A. Napoli, A. Rashidinejad, S. Ranzini, S. Erkilinc, A. Kakkar, A. Mathur, V. Dominic, P. Samra, H. Sun, A. Somani, and D. Welch, "DSP design for point-to-multipoint transmission," *in Proceedings Optical Fiber Communication Conference (OFC 2023)*, San Diego, USA, paper W1E.1, DOI: Not available.

[6] E. P. da Silva and D. Zibar, "Widely linear blind adaptive equalization for transmitter IQ-imbalance/skew compensation in multicarrier systems," *in Proceedings European Conference on Optical Communication (ECOC 2016)*, Dusseldorf, Germany, 2016, paper M.1.B.5, DOI: Not available.

[7] G. Bosco, S. M. Bilal, A. Nespola, P. Poggiolini, and F. Forghieri, "Impact of the transmitter IQ-skew in multi-subcarrier coherent optical systems," *in Proceedings Optical Fiber Communications Conference and Exhibition (OFC 2016)*, Anaheim, CA, USA, 2016, paper W4A.5, DOI: 10.1364/ofc.2016.w4a.5.

[8] H. Chen, X. Su, Z. Tao, T. Oyama, H. Nakashima, T. Hoshida, and K. Kato, "An accurate and robust in-phase/quadrature skew measurement for coherent optical transmitter by image spectrum analyzing," *in Proceedings European Conference on Optical Communication (ECOC 2017)*, Gothenburg, Sweden, 2017, paper P1.SC3.35, DOI: 10.1109/ECOC.2017.8345918.

[9] C. Ju, Z. Tao, Y. Fan, Y. Zhao, H. Chen, X. Su, and T. Hoshida, "Calibration of in-phase/quadrature amplitude and phase response imbalance for coherent receiver," *in Proceedings Optical Fiber Communications Conference and Exhibition (OFC 2017)*, Los Angeles, USA, 2017, paper W2A.55, DOI: 10.1364/OFC.2017.W2A.55.

[10] E. P. da Silva and D. Zibar, "Widely linear equalization for IQ imbalance and skew compensation in optical coherent receivers," *Journal of Lightwave Technology*, vol. 34, no. 15, pp. 3577-3586, 2016, DOI: 10.1109/JLT.2016.2577716.

[11] M. Arikawa, M. Sato, and K. Hayashi, "Compensation and monitoring of transmitter and receiver impairments in 10,000-km single-mode fiber transmission by adaptive multi-layer filters with augmented inputs," *Optics Express*, vol. 30, no. 12, pp. 20333-20359, 2022, DOI: 10.1364/OE.459959.